Model of temperature quenching of photoluminescence in disordered semiconductors and comparison to experiment

O. Rubel,* S. D. Baranovskii, K. Hantke, B. Kunert, W. W. Rühle, P. Thomas, K. Volz, and W. Stolz
Faculty of Physics and Material Sciences Center, Philipps Universität Marburg, Renthof 5, D-35032 Marburg, Germany
(Received 29 November 2005; published 6 June 2006)

A phenomenological model is suggested to describe nonradiative recombination of optical excitations in disordered semiconductor heterostructures. The general property of disordered materials is a strong decay of the photoluminescence intensity with rising temperature. We show that this temperature dependence is a consequence of the interplay between radiative and nonradiative recombination and hopping dynamics of excitations in the manifold of localized states created by disorder potential. The dynamics is studied by kinetic Monte Carlo simulations. Experimental data on the thermal quenching of the photoluminescence intensity in (GaIn)(NAs)/GaAs and Ga(NAsP)/GaP quantum wells are presented, which are in good agreement with the theoretical results.

For all disordered materials, it has been well-established that the quantum efficiency of the photoluminescence (PL) drastically decreases with increasing temperature. Classical theoretical approaches to description of nonradiative processes in perfect crystalline semiconductors are not applicable to disordered materials, since the behavior of photoexcited electrons and holes in the latter systems is essentially determined by disorder potential that causes spatial localization of electron states. We suggest in this Brief Report a model of nonradiative recombination in disordered materials, which takes into account not only the interplay between radiative and nonradiative processes, but also the dynamic exchange of charge carriers between localized states. We show that these dynamic effects determine the thermal quenching of the PL at low temperatures. Furthermore, we show how the temperature dependence of the PL intensity $I(T)$ is related to important parameters of disordered materials, such as the localization energy scale and the relative concentration of nonradiative centers and traps.

Although our model is general and it can be applied to any disordered system, we test it here on a particular case of semiconductor heterostructures containing nitrogen, which are currently intensively studied for applications in optical communications and photovoltaics. Materials containing nitrogen suffer from disorder effects, which become more pronounced with increasing of the nitrogen content. At room temperature, the majority of generated electrons and holes recombine nonradiatively. This leads to unfavorably high threshold current densities in lasers and to an unfavorably short minority carrier diffusion length in solar cells.

We studied experimentally the thermal quenching of the PL in $Ga_{0.7}In_{0.3}N_{0.006}As_{0.994}/GaAs$ and in $GaN_{0.04}As_{0.80}P_{0.16}/GaP$ quantum wells (QWs). The PL measurements were performed under direct excitation of QWs with a Ti:sapphire laser with the wavelength of 800 nm in a continuous wave (cw) regime for Ga(NAsP)/GaP QWs and using a short pulse excitation with the wavelength of 900 nm for (GaIn)(NAs)/GaAs QWs. The excitation density was 14 W cm^2 in the short pulse regime. The sample temperature in the cold-finger cryostat was varied from 10 K to room temperature. For cw measurements, the PL signal was dis-

persed in a 1 m grating monochromator (THR 1000 from Jobin-Yvon) and collected by a cooled germanium detector applying the standard lock-in technique. For the short pulse measurements, the PL signal was dispersed by a 32 cm spectrometer with a spectral resolution of 2 nm and detected using a Hamamatsu S1 streak camera with a time resolution of 20 ps. Time-integrated PL intensities $I(T)$ are discussed below.

Experimentally obtained $I(T)$ dependences are shown in Fig. 1. The prominent features of the temperature-induced quenching of the PL are the relatively weak (nonexponential) temperature dependence at low temperatures, succeeded by a steep drop by several orders of magnitudes and subsequent saturation of the PL. This shape of the thermal quenching of
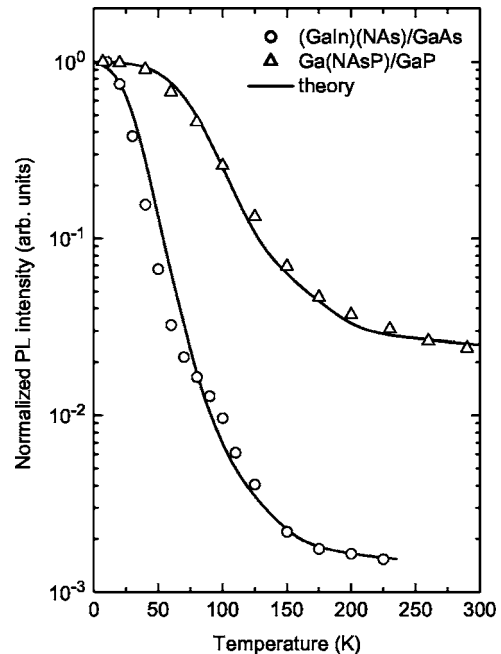
FIG. 1. Experimental data for the normalized PL intensity (I/I_0) as a function of temperature for $Ga_{0.7}In_{0.3}N_{0.006}As_{0.994}/GaAs$ and $GaN_{0.04}As_{0.80}P_{0.16}/GaP$ QWs (symbols). Solid lines show the results of the kinetic Monte Carlo simulation.

the PL is generally observed in disordered systems, e.g., (GaIn)(NAs) QWs,[1–3] Ga(AsSbN) QWs,[4] InGaAs/InAlAs superlattices,[5] and (InGa)N/GaN QWs.[6–8]

Numerous attempts have been devoted to the theoretical interpretation of the PL temperature dependence of the kind shown in Fig. 1. These attempts differ by the attribution of nonradiative channels to different physical processes. For example, it was shown that in (GaIn)As/GaAs QWs with shallow quantized states, the nonradiative recombination is related to the thermal activation of optical excitations from the radiative states in the well into the barriers.[9] This mechanism cannot, however, account for $I(T)$ dependence in (GaIn)(NAs) QWs with large band offsets. Traditionally non-radiative recombination is associated with thermal activation of excitations from radiative states into nonradiative channels.[10–12] Up to three distinct activation energies for nonradiative processes have been suggested. Numerous optical measurements, however, evidence a continuous energy distribution of states in band tails, which is hardly compatible with a few discrete levels responsible for the activation energies.

Grenouillet et al.[1] pointed out the similarity between thermal quenching of the PL intensity in (GaIn)(NAs) QWs and that in amorphous semiconductors, such as chalcogenide glasses and amorphous silicon.[13] In amorphous semiconductors one can resolve a temperature range where $I(T)$ follows the dependence

$$I \propto \exp(-T/T_1) \qquad (1)$$

with some characteristic temperature T_1. Gee and Kastner[14] showed that this expression can be obtained assuming that energy barriers for nonradiative processes have an exponential distribution, though they did not specify the origin of this distribution. Baranovskii and Karpov[15] ascribed this exponential distribution of barriers to the exponential energy dependence of capture cross section of carriers into localized states, while Street[13] ascribed the distribution of barriers to the exponential density of states in the band tails. Previous approaches were based on the assumption that carriers captured into some localized states either recombine from these particular states radiatively, or the carriers are thermally released into nonradiative channels. A possibility of the redistribution of carriers between radiative states has been evidenced experimentally in numerous studies[16–18] and we suggest below a model that takes this dynamics into account. Furthermore, we show that only taking into account the redistribution of excited carriers between localized states prior to the radiative or nonradiative recombination, one can explain the observed $I(T)$ dependences in the whole temperature range.

The model of the PL looks as follows. Electrons and holes generated by optical excitation are captured into localized states created by the disorder potential and called here trapping sites, which are centers of radiative recombination. These sites are assumed randomly distributed in space and energy forming the so-called band tails, which are characterized by density of states $g(\epsilon)$ [Fig. 2(a)].

We consider the case of strongly correlated electron-hole
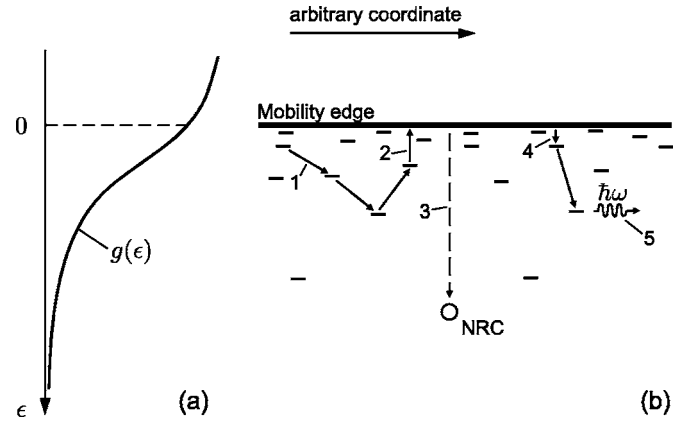
FIG. 2. (a) Schematic energy distribution of localized states in the band tail. The origin of the energy axes is set to the mobility edge. (b) Schematic illustration of the kinetic processes involved in the model of exciton dynamics: 1—hopping transitions between localized states, 2—thermal activation to the mobility edge, 3—capture to nonradiative centers (NRC), 4—retrapping, and 5—radiative recombination.

pairs in the form of excitons, assuming that such pairs can be localized with respect to their center-of-mass coordinate. Excitons can either perform transitions between localized states or they can be thermally released into extended states above the mobility edge. Being excited to the mobility edge, excitons can either be captured by nonradiative centers or they can be recaptured into radiative trapping sites. These processes are schematically illustrated in Fig. 2(b). We will show below that these processes are decisive for the shape of the dependence $I(T)$.

The phonon-assisted hopping transitions between localized states are described by Miller-Abrahams tunneling rates[19]

$$\nu_{ij} = \nu_0 \exp\left(-\frac{2r_{ij}}{\alpha} - \frac{\epsilon_i - \epsilon_j + |\epsilon_i - \epsilon_j|}{2k_B T}\right), \qquad (2)$$

where ϵ_i and ϵ_j are energies of sites i and j, respectively, r_{ij} is the intersite distance, α is the decay length of the localized exciton center-of-mass wave function, ν_0 is the attempt-to-escape frequency, and k_B is the Boltzmann constant. The thermal activation from a localized state with energy ϵ to the mobility edge is determined by the rate

$$\nu_a = \nu_0 \exp(-\epsilon/k_B T). \qquad (3)$$

For those excitons which are activated to the mobility edge, the probability to recombine nonradiatively is determined by the ratio of the concentration of nonradiative centers N_{nr} to the sum concentration $(N_{nr}+N_t)$ of nonradiative centers and traps, provided the traps and nonradiative centers have the same capture cross section. If the capture cross sections of radiative and nonradiative centers are different, one can easily modify the results by weighing the concentrations N_t and N_{nr} with the corresponding capture cross sections. The radiative rate is defined as the inverse exciton lifetime τ_0^{-1}. The quantum efficiency is determined by the ratio between the number of excitons that recombine radiatively and the total

number of generated excitons. For simulations we have essentially modified the algorithm suggested in Ref. 20 in order to account for nonradiative processes as described above.

We verify the suggested model by comparing its results with experimental data in Fig. 1. For simulations we choose the exponential energy distribution of localized states

$$g(\epsilon) = \epsilon_0^{-1} \exp(-\epsilon/\epsilon_0) \qquad (4)$$

with a characteristic energy ϵ_0 as proven for (GaIn)(NAs) QWs.[17,18,21] The results of the computer simulations are shown by solid lines in Fig. 1. Known values of the material parameters $\epsilon_0 = 8$ meV, $N_t\alpha^2 = 0.1$, $\nu_0\tau_0 = 10^4$ were taken for (GaIn)(NAs) QWs.[17,18,21] For Ga(NAsP) QWs the parameters were $\epsilon_0 = 10$ meV, $N_t\alpha^2 = 0.01$, and $\nu_0\tau_0 = 5 \times 10^4$. The ratios $N_{nr}/(N_{nr}+N_t) = 0.12$ and 1.4×10^{-3} were necessary in order to fit the experimental data for (GaIn)(NAs) and Ga(NAsP) QWs, respectively.

The conclusions to be deduced from the agreement between the results of the Monte Carlo simulation and the experimental data in Fig. 1 are the following. First, the considered model contains physical mechanisms which are necessary in order to account for the observed temperature dependence of the PL intensity in the whole temperature range. Second, a comparison between the results of computer simulation carried out in the frame of the formulated model provides important information on material parameters, such as the ratio between concentrations of nonradiative and radiative centers $N_{nr}/(N_{nr}+N_t)$ and the energy scale ϵ_0.

However, these conclusions might be of little help to experimentalists, who measure $I(T)$ dependences and would like to deduce material parameters without carrying out elaborate computer simulations. Below we provide an analytical description of $I(T)$ in order to gain better understanding of the important physical mechanisms and to supply experimentalists with a recipe of how to determine such parameter as, for instance, $N_{nr}/(N_{nr}+N_t)$ and ϵ_0 from the experimental data using analytical formulas. One should bear in mind, however, that the analytical description can be carried out only in the frame of a simplified model. The simplification is introduced on the expense of neglecting the energy relaxation of recombining carriers prior to recombination events. The model can be formulated on the base of the one suggested by Gee and Kastner,[14] if one assumes that an exciton thermally activated to the mobility edge does not necessarily recombine nonradiatively, but can be recaptured into a radiative state with probability $N_t/(N_{nr}+N_t)$. Then the approach of Gee and Kastner[14] yields the temperature dependence of the PL quantum efficiency in the form

$$I = I_0 \int_0^\infty d\epsilon\, g(\epsilon) \left[1 + \nu_0\tau_0 \frac{N_{nr}}{N_{nr}+N_t} \exp(-\epsilon/k_B T) \right]^{-1}, \quad (5)$$

were I_0 is the quantum efficiency at zero temperature. In the limit of very low temperatures, $k_B T \ll \epsilon_0$, this formula can be reduced to the form of Eq. (1) with the characteristic temperature T_1 related to the material parameters as

$$T_1 = \epsilon_0 k_B^{-1} \ln^{-1}\left(\nu_0\tau_0 \frac{N_{nr}}{N_{nr}+N_t} \right). \qquad (6)$$
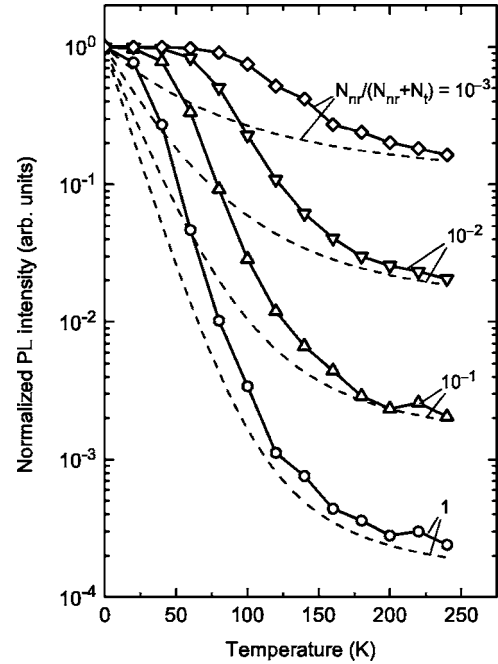
FIG. 3. Comparison between the results of Monte Carlo simulations (solid lines) and those of Eq. (5) (dashed lines).

Results for the quantum efficiency as a function of temperature obtained from Eq. (5) are compared in Fig. 3 with the results of the straightforward Monte Carlo simulations for the experimentally relevant parameters: $\epsilon_0 = 10$ meV, $N_t\alpha^2 = 0.5$, and $\nu_0\tau_0 = 10^4$. The results of the simplified analytical theory essentially deviate from those of computer simulations at low temperatures, while at high temperatures a good agreement is established. The reason for these trends is rather transparent. At low temperatures, excitons trapped into localized states perform energy-loss hopping transitions between the traps. Concomitantly, the energy distribution of excitons shifts towards deeper states in the band tail with respect to the mobility edge. Hence the activated nonradiative recombination becomes weaker as compared to that given by Eq. (5), in which it was implicitly assumed that excitations are frozen after the first capture event and no dynamical exchange between traps is allowed. As temperature increases and becomes comparable with the energy scale of the band tail ($T \approx \epsilon_0/k_B$), the thermal release to the mobility edge becomes efficient and the intersite dynamics does not play an essential role anymore. Then the energy distribution of excitons approaches $g(\epsilon)$. This explains why the PL intensities obtained from the Monte Carlo simulations are close to those obtained from Eq. (5) at high temperatures.

Apparent agreement between the analytical results and computer simulations at high temperatures suggests this temperature range as convenient for interpretation of experimental data. At temperatures above ~ 150 K, the quantum efficiency in Fig. 3 approaches its asymptotic value $I/I_0 \approx [1 + N_{nr}\nu_0\tau_0/(N_{nr}+N_t)]^{-1}$. We would like to emphasize that the level of the high-temperature plateau in the $I(T)$ dependence provides the straightforward estimate for the combination of material parameters $N_{nr}\nu_0\tau_0/(N_{nr}+N_t)$. Although such high-temperature plateaus were observed in numerous experimen-

tal studies,[1–3] they have not received the necessary attention yet.

Instead more attention of researchers has been paid to the magnitude of the characteristic temperature T_1 in Eq. (1). Equation (6) can be indeed considered as a useful approximation that relates T_1 to the material parameters. For example, taking the value $T_1 = 17$ K[1,3] and estimating $N_{nr}\nu_0\tau_0/(N_{nr}+N_t) \approx 10^3$ from the high-temperature plateaus in the $I(T)$ dependences for (GaIn)(NAs) QWs,[1,3] one comes via Eq. (6) to the very reasonable estimate $\epsilon_0 \approx 10$ meV. However, one should keep in mind that the real shape of $I(T)$ given by the simplified analytical theory differs essentially from the result of computer simulations particularly at low temperatures, as well seen in Fig. 3. While analytical theory predicts a steep drop of the $I(T)$ curve at very low temperatures, the results of the kinetic Monte Carlo simulations demonstrate a much weaker temperature dependence at low temperatures as observed experimentally. The latter is caused by the dynamical redistribution of excitations towards deeper states in the band tail at low temperatures, which hinders their nonradiative recombination via activation to the mobility edges.

*Email address: oleg.rubel@physik.uni-marburg.de

[1] L. Grenouillet, C. Bru-Chevallier, G. Guillot, P. Gilet, P. Duvaut, C. Vannuffel, A. Million, and A. Chenevas-Paule, Appl. Phys. Lett. **76**, 2241 (2000).

[2] A. Polimeni, M. Capizzi, M. Geddo, M. Fischer, M. Reinhardt, and A. Forchel, Appl. Phys. Lett. **77**, 2870 (2000).

[3] H. D. Sun, M. Hetterich, M. D. Dawson, A. Y. Egorov, D. Bernklau, and H. Riechert, J. Appl. Phys. **92**, 1380 (2002).

[4] J. Li, S. Iyer, S. Bharatan, L. Wu, K. Nunna, W. Collis, K. K. Bajaj, and K. Matney, J. Appl. Phys. **98**, 013703 (2005).

[5] L. C. Pocas, E. M. Lopes, J. L. Duarte, I. F. L. Dias, S. A. Lourenco, E. Laureto, M. Valadares, P. S. S. Guimaraes, L. A. Cury, and J. C. Harmand, J. Appl. Phys. **97**, 103518 (2005).

[6] M. Ichimiya, T. Hayashi, M. Watanabe, T. Ohata, and A. Ishibashi, Phys. Status Solidi A **199**, 347 (2003).

[7] K. S. Ramaiah, Y. K. Su, S. J. Chang, B. Kerr, H. P. Liu, and I. G. Chen, Appl. Phys. Lett. **84**, 3307 (2004).

[8] J.-H. Chen, Z.-C. Feng, H.-L. Tsai, J.-R. Yang, P. Li, C. Wetzel, T. Detchprohm, and J. Nelson, Thin Solid Films **498**, 123 (2006).

[9] G. Bacher, H. Schweizer, J. Kovac, A. Forchel, H. Nickel, W. Schlapp, and R. Lösch, Phys. Rev. B **43**, 9312 (1991).

[10] I. A. Buyanova, M. Izadifard, W. M. Chen, A. Polimeni, M. Capizzi, H. P. Xin, and C. W. Tu, Appl. Phys. Lett. **82**, 3662 (2003).

[11] I. A. Buyanova, W. M. Chen, and C. W. Tu, Solid-State Electron. **47**, 467 (2003).

[12] R. J. Potter and N. Balkan, J. Phys.: Condens. Matter **16**, S3387 (2004).

[13] R. A. Street, *Hydrogenated Amorphous Silicon* (Cambridge University Press, Cambridge, England, 1991).

[14] C. M. Gee and M. Kastner, Phys. Rev. Lett. **42**, 1765 (1979).

[15] S. D. Baranovskii and V. G. Karpov, Sov. Phys. Semicond. **18**, 828 (1984).

[16] T. K. Ng, S. F. Yoon, S. Z. Wang, L. H. Lin, Y. Ochiai, and T. Matsusue, J. Appl. Phys. **94**, 3110 (2003).

[17] H. Grüning, K. Kohary, S. D. Baranovskii, O. Rubel, P. J. Klar, A. Ramakrishnan, G. Ebbinghaus, P. Thomas, W. Heimbrodt, W. Stolz *et al.*, Phys. Status Solidi C **1**, 109 (2004).

[18] O. Rubel, M. Galluppi, S. D. Baranovskii, K. Volz, L. Geelhaar, H. Riechert, P. Thomas, and W. Stolz, J. Appl. Phys. **98**, 063518 (2005).

[19] A. Miller and E. Abrahams, Phys. Rev. **120**, 745 (1960).

[20] S. D. Baranovskii, R. Eichmann, and P. Thomas, Phys. Rev. B **58**, 13081 (1998).

[21] R. A. Mair, J. Y. Lin, H. X. Jiang, E. D. Jones, A. A. Allerman, and S. R. Kurtz, Appl. Phys. Lett. **76**, 188 (2000).